JSHC
Japan Society of
Histochemistry and Cytochemistry
Established 1959

Acta Histochem. Cytochem. 55 (4): 111–118, 2022
doi: 10.1267/ahc.22-00018

Regular Article

Morphologic Analysis of M2 Macrophage in Glioblastoma: Involvement of Macrophage Extracellular Traps (METs)

Ayano Michiba[1], Kazuya Shiogama[2], Tetsuya Tsukamoto[1], Masaya Hirayama[2], Seiji Yamada[1] and Masato Abe[2]

[1]Department of Diagnostic Pathology, Fujita Health University Graduate School of Medicine and [2]Department of Morphology and Pathology, Fujita Health University Medical Science, 1–98 Dengakugakubo, Kutsukake-cho, Toyoake, Aichi 470–1192, Japan

Received February 17, 2022; accepted July 1, 2022; published online August 10, 2022

Macrophages are classified into two phenotypes, M1 and M2, based on their roles. M2 macrophages suppress inflammation and increase in proportion to the malignancy of brain tumors. Recently, macrophage extracellular traps (METs), which change into a network, have been reported as a unique form of macrophage cell death. In this study, immunohistochemical analysis of macrophages in METs in human glioblastoma was performed. To distinguish between M1 and M2 macrophages, multiple immunostainings with Iba1 combined with CD163 or CD204 were performed. M2 macrophages were present in small amounts in normal and borderline areas but showed an increasing trend as they shifted to tumor areas, and most of them were the activated- or phagocytic-type. We also successfully detected METs coexisting with fibrin and lactoferrin near the border between the tumor and necrotic area. M2 macrophages not only suppressed inflammation but also were involved in the formation of METs. This study found that M2 macrophages play various roles in unstable situations.

Key words: M1 and M2 macrophage, microglia, glioblastoma, macrophage extracellular traps (METs)

I. Introduction

Macrophages are classified into two phenotypes, namely, M1 macrophages, the proinflammatory, and M2 macrophages, the anti-inflammatory, and switch between the two states depending on environmental factors at the site [10, 11, 19]. M1 macrophages are activated by IFN-γ and produced proinflammatory cytokines to kill bacteria, whereas M2 macrophages are involved in the production of various angiogenic and anti-inflammatory factors, such as IL-10, TGF-β, and prostaglandin E2, and the promotion of regulatory T-cell infiltration [32]. Several markers, have been used to detect macrophages immunohistochemically, and some studies reportedly detected M1 and M2 macrophage systems. However, M1 and M2 macrophages cannot be differentiated clearly [2, 5, 14, 16, 18, 19, 25, 28, 30].

Microglia, which have phagocytic functions, are present in the brain and are referred to as "brain macrophages." They are known to change their shape into three types depending on their active state: ramified-, activated-, and phagocytic-type [22, 30]. In the normal state, ramified-type microglia were the most common, with small, branched, elongated dendrites and little cytoplasm. In the case of a disease condition, the shape of macrophages changes from the ramified-type to activated-type with residual dendrites and phagocytic-type macrophages that are round and lost their dendrites [30]. Thus, macrophages change their form and function in response to the environment and function as sensors that reflect the biological condition in real-time.

The number of newly diagnosed glioma cases in Japan is approximately 4,000–5,000 per year, the most frequently diagnosed malignant brain tumor, accounting for about

Correspondence to: Tetsuya Tsukamoto, Department of Diagnostic Pathology, Fujita Health University Graduate School of Medicine, 1–98 Dengakugakubo, Kutsukake-cho, Toyoake, Aichi 470–1192, Japan.
E-mail: ttsukamt@fujita-hu.ac.jp

Table 1. *Primary antibodies*

Name	Clone	Make	Dilution	Antigen retrieval	
Pan Macrophage					
CD68	KP1	Dako	400	20 mg/ml proteinase K solution	room temperature
Iba1 (Ionized Calcium Binding Adaptor Molecule 1)	—	Wako	2,000	1 mM EDTA solution (pH 8.0)	pressure cooker
M1 Macrophage					
CD80	EPR1157 (2)	Abcam	2,000	10 mM citrate buffer solution (pH 6.0)	pressure cooker
M2 Macrophage					
CD163	10D6	Abcam	100	10 mM citrate buffer solution (pH 6.0)	pressure cooker
CD204	SRA-E5	Trans Genic Inc	2,000	1 mM EDTA solution (pH 8.0)	pressure cooker
Neutrophil					
NE (neutrophil elastase)	—	Abcam	2,000	10 mM citrate buffer solution (pH 6.0)	pressure cooker
MPO (Myeloperoxidase)	—	Dako	10,000		
Lactoferrin	—	Gen Way	300	10 mM citrate buffer solution (pH 6.0)	pressure cooker
Ets					
Cit-H3 (Citrullinated Histone H3)	—	Abcam	900	10 mM citrate buffer solution (pH 6.0)	pressure cooker
Others					
FGG (Fibrinogen Gamma chain)	1F2	Abnova	2,000	10 mM citrate buffer solution (pH 6.0)	pressure cooker
CD31	1A10	Novocastra	100	10 mM citrate buffer solution (pH 6.0)	pressure cooker

30% of all cases [29]. Glioblastoma, a tumor classified as grade IV and the most common malignant tumor in the World Health Organization classification, has an extremely poor prognosis, usually resulting in death within 2 years. Treating it with surgical resection alone is difficult due to the nature of tumor cells invading the normal brain, and thus, the treatment is combined with radiotherapy and chemotherapy.

Recently, M2 macrophages have been reported to increase in proportion to the malignancy of glioma, and M2 macrophage infiltration has been shown as an indicator of malignancy [32]. It has been demonstrated *in vitro* that repolarization of M2 macrophages and conversion to M1 macrophages can suppress cancer progression [6, 11, 15, 16, 21, 23, 36].

In 2004, neutrophil extracellular traps (NETs) were discovered, in which neutrophils sacrifice their cells and transform into a network to capture extracellular foreign substances [3]. NETs not only kill the captured foreign substances through antimicrobial granules but also promote phagocytosis through neutrophils and macrophages. This phenomenon has been defined as "NETosis," a cell death unique for neutrophils that is neither apoptosis nor necrosis. Recently, macrophage extracellular traps (METs), which cause similar cell death in macrophages, have been reported [1, 12]. They are involved in some diseases. However, many unknowns remain, especially on the association of NETs and METs with malignant tumors, which have rarely been analyzed in detail [1, 8, 17, 20, 24, 35].

In this study, a detection system was established to differentiate M1 and M2 macrophages in glioblastoma using immunohistochemical techniques. Further, the detection system was used to morphologically analyze the location and shape changes in each region of microglia and macrophages in glioblastoma. Finally, immunohistochemical analysis using various NETs and METs markers was performed to confirm whether NETs and METs are involved in glioblastoma or not.

II. Materials and Methods

Case selection

Fifteen formalin-fixed paraffin-embedded blocks of glioblastoma surgically removed at Fujita Medical University Hospital from 2016 to 2019 were used in this study. The Research Ethics Review Committee of Fujita Medical University approved the use of the clinical samples for this study (No. CI20-086).

Immunostaining for macrophage subclassification

Primary antibodies are listed in Table 1. Xylene and alcohol were used to deparaffinize and hydrophilize thinly sliced formalin-fixed paraffin sections. Endogenous peroxidase activity was blocked in methanol with 0.03% hydrogen peroxide for 30 min at room temperature. Primary antibodies were allowed to react overnight at room temperature after antigen retrieval. An amino acid polymer reagent (Histone Simple Stain MAX-PO: Nichirei) reacted for 30 min at room temperature. The antibody was colorized with 3,3'-diaminobenzidine tetrahydrochloride (Dako, Redox, Romania: DAB). Nuclear staining was performed using Mayer's hematoxylin.

For immune-multiplex staining, a cocktail of primary antibodies, anti-Iba1, and anti-CD163 antibodies, was reacted overnight at room temperature. As secondary antibodies, anti-mouse IgG antibody (Histofine Simple Stain MAX-PO(M): Nichirei) and anti-rabbit IgG antibody (Histofine Simple Stain AP(R): Nichirei) were reacted for 30 min at room temperature. Nuclear staining was performed using the nuclear fast red. For fluorescence multiplex staining, a cocktail of primary antibodies, anti-Cit-H3, and anti-CD204 antibodies, was also reacted overnight.

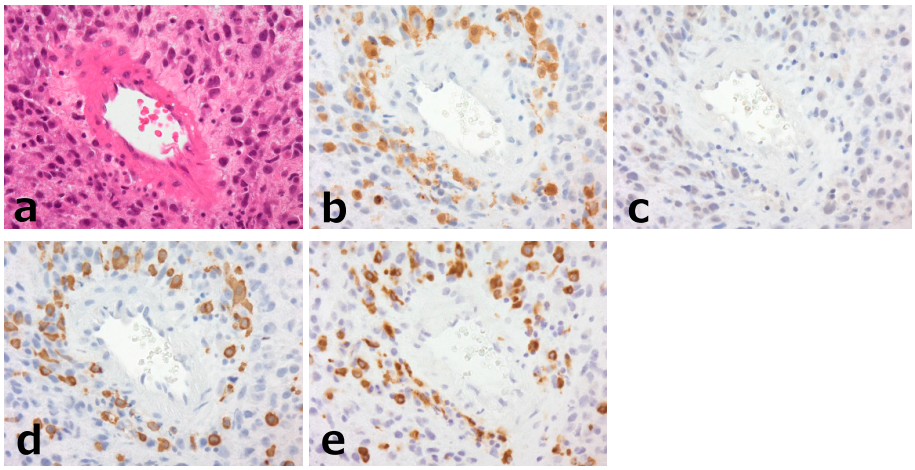

Fig. 1. Immunostaining images using macrophage markers in glioblastoma. HE (**a**), Iba1 (**b**), CD80 (**c**), CD163 (**d**), CD204 (**e**). Iba1, CD163, and CD204 were positive for macrophages (**c, e, f**), whereas CD80 was weakly positive (**b, d**). Original magnification 400× (**a–f**).

Secondary antibodies cocktail with Alexa Fluor 568-conjugated anti-mouse IgG antibody (diluted 300-fold, Thermo Fisher Scientific) and Alexa Fluor 488-conjugated anti-rabbit IgG antibody (diluted 300-fold, Thermo Fisher Scientific) were combined and added with DNA 4',6-diamidino-2-phenylindole (diluted 1,000-fold, Thermo Fisher Scientific: DAPI) and reacted for 30 min.

Classification of macrophages in regions

Three reagions were identified: normal area, boundary area (boundary between massive tumor and areas of low cell density), and tumor area contained in the same section. Tumor area were futher classified into three: around the normal blood vessels, tumor infiltration sites, and palisading necrosis. These five regions were used for the experiment.

Hemotoxylin and eosin (HE) stained and immuno-multiplexed specimens were used to take 20 images in each region (5 in all) with an upright microscope (Axio Imager 2, Carl Zeiss) at 400×. The ratio of M1 macrophages (positive only for Iba1) and M2 macrophages (positive for both Iba1 and CD163) were measured. The shape of macrophages was classified into three types: ramified-, activated-, and phagocytic-type, as reported by Sasaki [30]. Statistical analysis using the Chi-squared test (χ-square test) was used to compare the distribution and shape changes of macrophages by region.

III. Results

Examination of macrophage markers

Immunostaining results in glioblastoma showed that Iba1, CD163, and CD204 were expressed to the same extent (Fig. 1b, d, e), whereas CD80 was weakly positive and difficult to determine (Fig. 1c). These results indicate that Iba1, CD163, and CD204 are useful as macrophage markers.

Macrophage subclassification

In immune-multiplex staining, cells positive only for Iba1 were classified as M1 macrophages (Fig. 2a), and cells positive for Iba1 and CD163 were classified as M2 macrophages (Fig. 2b). No cells were positive for CD163 only. Macrophages were successfully classified into three shapes according to the presence or absence of dendrites and the size of the spores. Ramified-type macrophages had small spores and elongated dendrites (Fig. 2c). Activated-type macrophages were characterized by higher cell volume and shortened dendrites (Fig. 2d). Phagocytic-type macrophages completely lost their dendrites and had rounder cells than activated-type macrophages (Fig. 2e). Next, normal, boundary, and tumor areas were identified on HE-stained and immune-multiplexed specimens (Fig. 3). The boundary area, which is boundary between massive tumor and areas of low cell density (Fig. 3c, d). The tumor area focused on around the normal blood vessels (Fig. 3e, f), tumor infiltrates (Fig. 3g, h), and palisading necroses (Fig. 3i, j). Palisading necrosis refers to the area where tumor cells surround the necrosis and are arranged in a fence-like pattern. Macrophage subclassification in each region is shown in Figure 4. M1 macrophages were significant in normal and borderline areas, whereas M2 macrophages were significant in tumor areas ($p < 0.05$) (Fig. 4a).

Ramified-type macrophages were significantly more abundant in normal areas than in border and tumor areas.

Immunohistochemical detection of NETs and METs

Reticular structures were identified near the border between the tumor and necrotic area in 2 of 16 cases (Fig. 5a, b). Tumor cells surrounded the necrosis in this area as in palisading necrosis. However, the tumor cells were not arranged in a fence-like pattern, and the necrosis was larger than in palisading necrosis. Therefore, it is considered to be the area that does not fit into any of the categories in Fig. 3.

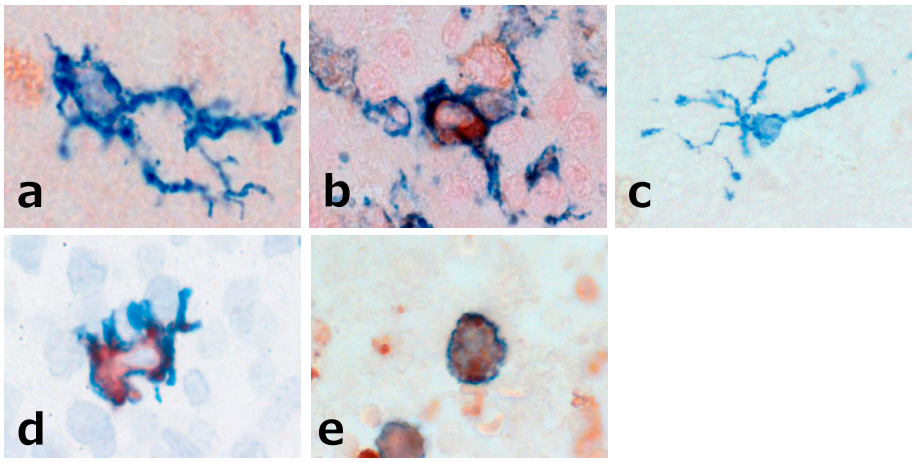

Fig. 2. Classification of macrophage types and shapes by immune-multiplex staining. The distinction between M1 and M2 macrophages using immune-multiplex staining. M1 macrophages were positive for Iba1 in dendrites (**a**), and M2 macrophages were positive for Iba1 in dendrites and CD163 in the cytoplasm (**b**). Ramified-type macrophages were small and had long dendrites (**c**). Activated-type macrophages had higher cell volume and shorter dendrites (**d**). Phagocytic-type macrophages lost their dendrites and became rounder than activated-type macrophages (**e**). Iba1: blue, CD163: brown. Original magnification 1000× (**a, b**).

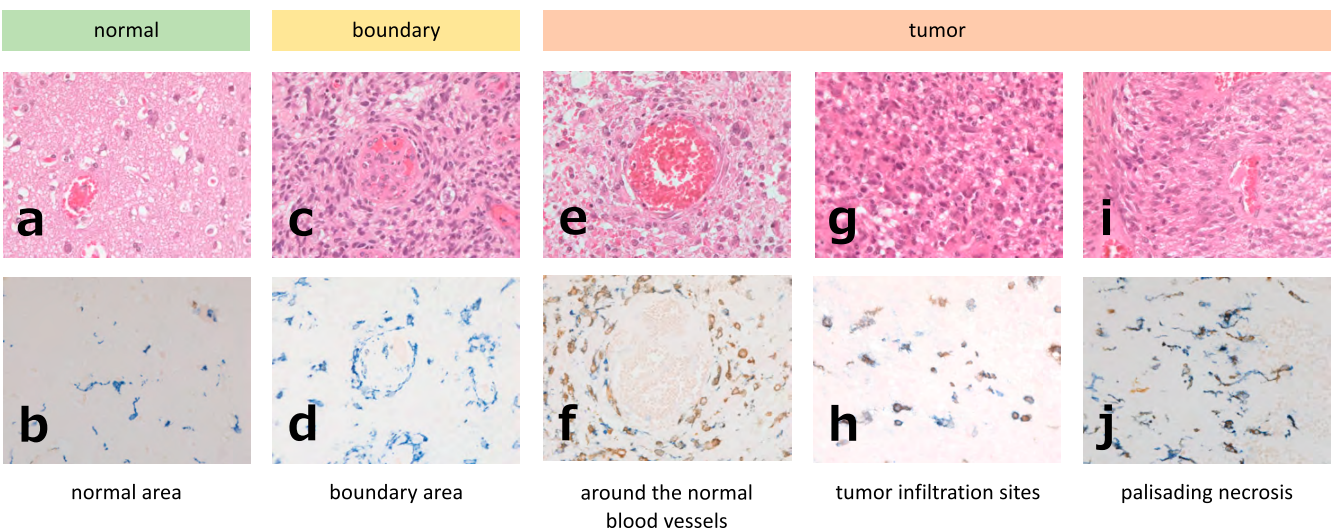

Fig. 3. Comparison between regions by HE staining and immune-multiplex staining. HE staining and immune-multiplex staining for Iba1 and CD163 were used to compare morphological features between regions. In the normal area, ramified-type M1 macrophages were observed sporadically (**b**). In the boundary area, a few activated- and phagocytic-type M1 macrophages were found in the periphery (**d**). In the tumor area, activated- and phagocytic-type M2 macrophages were predominantly observed (**f, h, j**).

Immunohistochemical staining in reticular formations is used to determine METs if Cit-H3 and macrophage markers are positive, and NETs if Cit-H3 and neutrophil markers are positive. Cit-H3 is a marker that detects histone proteins in nuclear components. The reticular formation we found in this study was positive for M2 macrophage markers CD163 and CD204, in addition for Cit-H3 (Fig. 5c–e). MPO and NE, the granule components of neutrophils, were both negative (Fig. 5f, g). Therefore, we concluded that the reticular formation we found in this study was METs. Furthermore, lactoferrin and FGG positively agree with the reticular structures (Fig. 5h, i). Because CD204 was more clearly expressed than CD163, CD204 was used in the fluorescence multiplex staining. Fluorescence multiplex staining for CD204, Cit-H3, and DAPI was shown (Fig. 5j–m). The nuclear components Cit-H3 and DAPI positively agreed with reticular structures, and CD204 was observed in the granular form attached to the reticular structures.

IV. Discussion

M2 macrophages are some of the aggravating factors in the tumor microenvironment, suppressing the inflammation and contributing to tumor growth, and have attracted much attention from the viewpoint of new cancer therapies. Although various macrophage markers have been used to

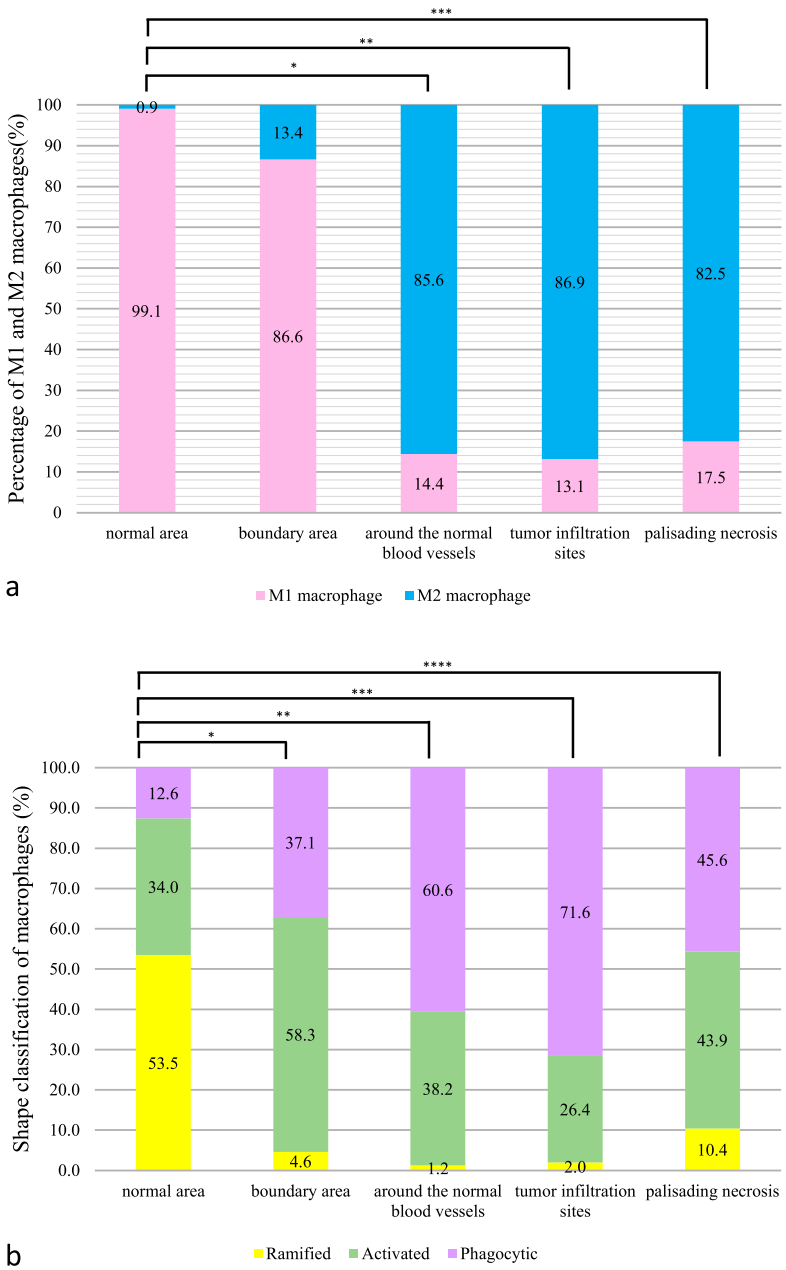

Fig. 4. Graphs showing the percentage of M1 and M2 macrophages and the shape classification of macrophages in each region. M1 macrophages were predominant in normal and boundary areas, whereas M2 macrophages were predominantly present in the tumor areas. More activated- and phagocytic-type macrophages were found in the boundary and tumor areas compared to normal areas (*: $p < 0.05$).

differentiate M1 and M2 macrophages, a detection system that can reliably differentiate them has not yet been established. In particular, selecting M1 macrophage markers is extremely difficult, a major problem that prevents the differentiation of M1 and M2 macrophages. In this study, Iba1, CD163, or CD204 was demonstrated to be useful for detecting macrophages in glioblastoma (Fig. 1c, e, f). Iba1 was positive for both macrophages and microglia in brain tissues, reconfirming its position as a pan-macrophage marker. M2 macrophage markers, CD163 and CD204, showed clear positive signals, whereas CD80, expected to be an M1 macrophage marker, failed to capture a positive signal in any cases and did not provide a fundamental solution (Fig. 1d). The method that differentiates M1 and M2 macrophages found in this study is immune-multiplex staining with Iba1 combined with CD163 or CD204 (Fig. 2). In other words, Iba1-positive and CD163- or CD204-negative can be regarded as M1 macrophages, and Iba1-positive and CD163- or CD204-positive as M2 macrophages. Since no Iba1-negative CD163 or CD204 positive pattern was observed, the two can be reliably differentiated using Iba1 as the main marker combined with

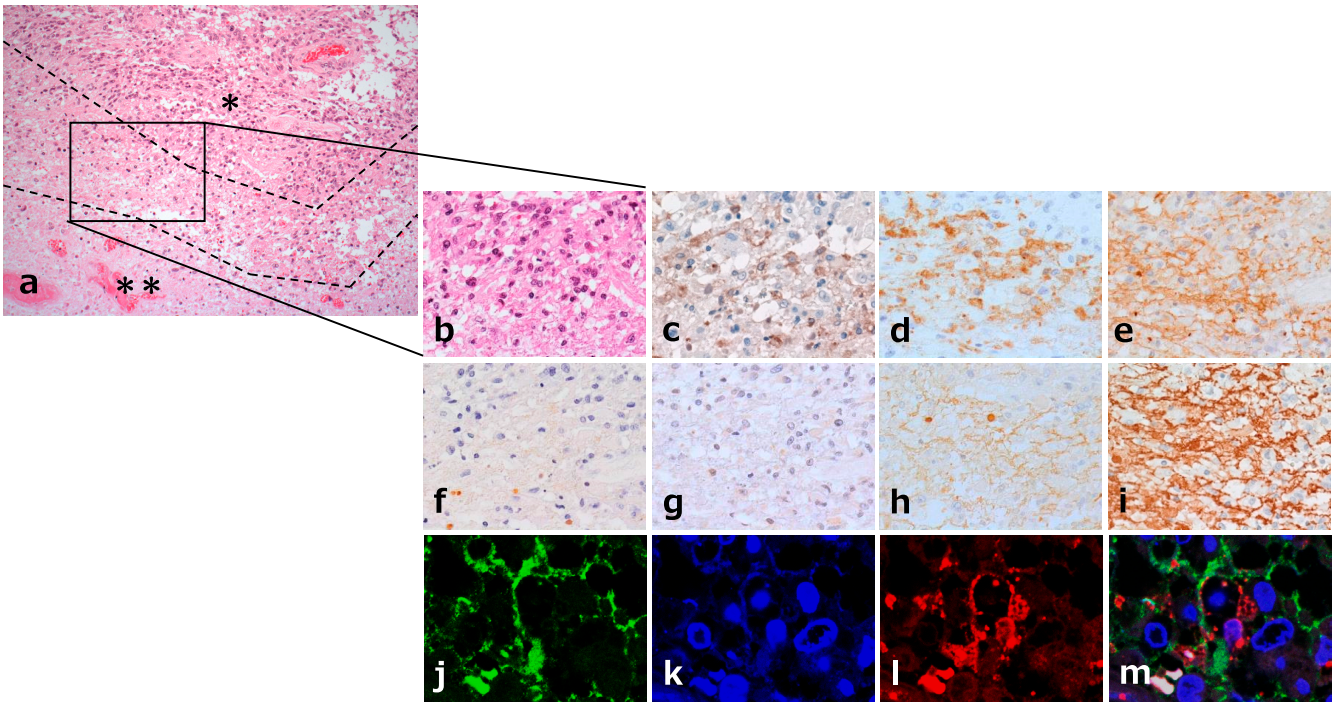

Fig. 5. Reticular structures and immunohistochemical analysis of METs in glioblastoma. Reticular structures were observed at the border between the tumor (*) and necrotic areas (**) (**a**). Enlarged views of the reticular structures were shown in (**b–m**). Immunohistochemically, the reticular structures were positive for CD163 (**c**), CD204 (**d**) and Cit-H3 (**e**), and negative for MPO (**f**) and NE (**g**). Lactoferrin (**h**) and FGG (**i**) were also positive. Fluorescence multiplex stainings for METs detection were shown in (**j–m**). Cit-H3 (**j**) and DAPI (**k**) were positive for reticular structures. CD204 (**l**) was observed in the granular form, and attached to the reticular structures (**m**) (merge). Original magnification 200× (**a**), 400× (**b–i**) and 630× (**j–m**).

M2 macrophage markers. Regarding the M1 and M2 macrophage ratio in each region of glioblastoma, most macrophages infiltrating the normal and borderline regions were M1 macrophages, whereas M2 macrophages were abundant in the tumor region (Fig. 4a). M2 macrophages showed an increasing trend as the tumor shifted from its normal appearance, proving once again that they are involved in tumor invasion.

Fourteen of the 15 cases were primary cases and one was a relapsed case. The percentage of M2 macrophages in the relapsed cases is shown below. The figures in parentheses indicate the mean percentage of M2 macrophages in all cases. Normal area 0% (0.9%), boundary area 0% (13.4%), around the normal blood vessels 59.8% (85.6%), tumor infiltration sites 80% (86.9%), Palisading necrosis was unclear and not measured. Compared to the overall population, relapsed cases generally had a lower percentage of M2 macrophages. However, since there was only one relapsed case, it was not possible to fully examine the results, and the significance of this result was determined to be unclear. Comparative study of primary and relapsed cases will be a future issue.

Conversely, the shape classification of each region revealed ramified-type as the most common in the normal area, whereas activated-type macrophages such as the activated- and phagocytic-types were more common in the boundary and tumor area (Fig. 4b). Although M2 macrophage infiltration in glioblastoma has already been reported, this study successfully established a method to differentiate M1 from M2 macrophages and to morphologically capture the active state of macrophages simultaneously. This method is useful for studies using clinical materials of brain tumors and is a versatile immunohistochemical technique that does not require special equipment.

METs are a form of cell death similar to NETs. The mechanisms of NETs and METs formation are described below. First, neutrophils and macrophages are activated by bacterial or other stimuli, disrupting the nuclear membrane. During nuclear membrane disruption, arginine in histone H3 is converted to citrulline through the action of peptidyl arginine deiminase 4 (PAD4), a nuclear protein citrullinating enzyme. This citrullination weakens the binding of histone H3 to DNA and causes chromatin to become fibrous. The nuclear component containing the citrullinated histone H3 spreads throughout the cytoplasm and fuses with the cytoplasmic component. Finally, they are morphed into reticular structures and extracellularly released to form NETs or METs [9, 26, 27, 34]. In the current study, M2 macrophage-derived METs were found near the border between the tumor and necrotic areas in two of 15 glioblastomas (Fig. 5). In our previous studies, neutrophil-derived NETs were involved in many inflammatory diseases and tumors [31]. Unlike neutrophils, macrophages can divide and proliferate at the site of infiltration, have a long life-

span, and have a high phagocytic capacity, suggesting that the frequency of METs formation is localized. Xu *et al.* claimed that immunohistochemical analysis of patients with non-functioning pancreatic neuroendocrine tumors showed that patients with high levels of tumor-infiltrating neutrophils or macrophages or positive NETs or METs expressions, had worse recurrence-free survival [37], suggesting that macrophages may morph into METs near the boundary between tumor and necrotic areas in glioblastoma to promote tumor invasion or necrosis. METs can also be used as a prognostic biomarker in glioblastoma, suggesting the possibility of targeting patients with glioblastoma. However, consistent with the reticular structures of METs, not only the cellular components of macrophages but also lactoferrin was positive in this study. Lactoferrin is contained in breast milk, saliva, and sweat and is known as an antibacterial agent that is also a granule component of neutrophils. Moreover, it is an important iron-binding glycoprotein that has been reported for its antitumor effects and also influences NETs formation [7, 13, 38]. Results of immunostaining in the METs region showed that MPO and NE in the cytoplasmic granules of neutrophils were negative, suggesting that lactoferrin is unlikely derived from neutrophils, is induced by another route, and then works as a biological defense function in cooperation with METs. When the outcome of all patients was examined, the two patients who developed METs had the best prognosis. The average life expectancy of glioblastoma is said to be 1.5 to 2 years, but these two cases survived for more than 3 years and 4 years and 7 months, respectively. The shortest survival time without METs was 2 months after diagnosis, and the longest survival time was 2 years and 8 months. From this, we speculated that the expression of METs may be involved in the suppression of tumor invasion. However, the number of cases was small and there was no significant difference between the two cases (P value: 0.2062, Kaplan-Meier method).

Furthermore, FGG, a fibrin marker, showed the same localization as METs. Our previous studies have shown that NETs and fibrin fibers coexist in many inflammatory diseases [31], and in METs, inflammation-induced fibrin exudates and forms NETs fibrous structures. Tamura *et al.* claimed that CD163-positive cells are lower at the tumor periphery brain zone than at the tumor core of glioblastoma [33]. In our study, CD163 and CD204 expression was similar except at the tumor periphery (Fig. 1d, e), but CD204 expression was higher than CD163 at the border between tumor and necrosis (i.e., tumor periphery) where METs were observed (Fig. 5c, d). Therefore, we used CD204 but not CD163 for fluorescent immunohistochemical staining. The observation of fluorescence multiple staining specimens of CD204, Cit-H3, and DAPI using confocal laser scanning microscope confirmed that METs are reticular structures with DNA components as a backbone and cellular components that adhered in a granular form. In addition, the nuclear component of METs was found more sensitive to Cit-H3 than DAPI, and a clearer image was obtained (Fig. 5j, k). Brinkmann *et al.* reported that detecting thin fibrous structures of NETs using DNA-binding dyes, such as DAPI and Hoechst, is difficult and recommended the use of Cit-H3 to prove the nuclear components of NETs and METs [4]. M2 macrophages are proinflammatory factors that increase with tumor infiltration and create a favorable cancer microenvironment for tumors. This is the first study that confirmed M2 macrophages are also involved in METs formation in glioblastoma. However, the mechanisms of METs' effects on tumors cannot be clearly defined. Due to the difficulty in clearly differentiating M1 and M2 macrophages and the fact that M1 and M2 macrophages can shift from one another, distinguishing them individually, including their functions, is difficult. However, M2 macrophages are indeed closely related to tumors, and thus, we will continue to investigate them in more detail based on the morphological findings obtained in this study.

Using immune-multiplex staining, this study demonstrated that quiescent M1 macrophages were transformed into active M2 macrophages upon tumor invasion on formalin-fixed paraffin sections. Immune-multiplex staining performed in this study may be applied to other studies of macrophage morphology in formalin-fixed paraffin sections. The presence of M2 macrophage-derived METs at the border between the tumor and necrotic areas of glioblastoma suggests that M2 macrophages not only suppress inflammation but also promote tumor invasion.

V. Conflicts of Interest

The authors declare that they have no conflicts of interest.

VI. References

1. Aulik, N. A., Hellenbrand, K. M. and Czuprynski, C. J. (2012) Mannheimia haemolytica and its leukotoxin cause macrophage extracellular trap formation by bovine macrophages. *Infect. Immun.* 80; 1923–1933.
2. Badylak, S. F., Valentin, J. E., Ravindra, A. K., McCabe, G. P. and Stewart-Akers, A. M. (2008) Macrophage phenotype as a determinant of biologic scaffold remodeling. *Tissue Eng. Part A.* 14; 1835–1842.
3. Brinkmann, V., Reichard, U., Goosmann, C., Fauler, B., Uhlemann, Y., Weiss, D. S., *et al.* (2004) Neutrophil extracellular traps kill bacteria. *Science* 303; 1532–1535.
4. Brinkmann, V., Abu Abed, U., Goosmann, C. and Zychlinsky, A. (2016) Immunodetection of NETs in Paraffin-Embedded Tissue. *Front. Immunol.* 7; 513.
5. Cherry, J. D., Olschowka, J. A. and O'Banion, M. K. (2014) Neuroinflammation and M2 microglia: the good, the bad, and the inflamed. *J. Neuroinflammation* 11; 98.
6. Coscia, M., Quaglino, E., Iezzi, M., Curcio, C., Pantaleoni, F., Riganti, C., *et al.* (2010) Zoledronic acid repolarizes tumour-associated macrophages and inhibits mammary carcinogenesis by targeting the mevalonate pathway. *J. Cell. Mol. Med.* 14; 2803–2815.
7. Dong, H., Yang, Y., Gao, C., Sun, H., Wang, H., Hong, C., *et al.*

(2020) Lactoferrin-containing immunocomplex mediates antitumor effects by resetting tumor-associated macrophages to M1 phenotype. *J. Immunother. Cancer* 8; e000339.
8. Doster, R. S., Rogers, L. M., Gaddy, J. A. and Aronoff, D. M. (2018) Macrophage Extracellular Traps: A Scoping Review. *J. Innate. Immun.* 10; 3–13.
9. Fuchs, T. A., Abed, U., Goosmann, C., Hurwitz, R., Schulze, I., Wahn, V., *et al.* (2007) Novel cell death program leads to neutrophil extracellular traps. *J. Cell Biol.* 176; 231–241.
10. Gordon, S. (2003) Alternative activation of macrophages. *Nat. Rev. Immunol.* 3; 23–35.
11. Hagemann, T., Lawrence, T., McNeish, I., Charles, K. A., Kulbe, H., Thompson, R. G., *et al.* (2008) "Re-educating" tumor-associated macrophages by targeting NF-kappaB. *J. Exp. Med.* 205; 1261–1268.
12. Hellenbrand, K. M., Forsythe, K. M., Rivera-Rivas, J. J., Czuprynski, C. J. and Aulik, N. A. (2013) Histophilus somni causes extracellular trap formation by bovine neutrophils and macrophages. *Microb. Pathog.* 54; 67–75.
13. Hu, L., Hu, X., Long, K., Gao, C., Dong, H. L., Zhong, Q., *et al.* (2017) Extraordinarily potent proinflammatory properties of lactoferrin-containing immunocomplexes against human monocytes and macrophages. *Sci. Rep.* 7; 4230.
14. Jiménez-Uribe, A. P., Valencia-Martínez, H., Carballo-Uicab, G., Vallejo-Castillo, L., Medina-Rivero, E., Chacón-Salinas, R., *et al.* (2019) CD80 Expression Correlates with IL-6 Production in THP-1-Like Macrophages Costimulated with LPS and Dialyzable Leukocyte Extract (Transferon®). *J. Immunol. Res.* 2019; 2198508.
15. Komohara, Y., Ohnishi, K., Kuratsu, J. and Takeya, M. (2008) Possible involvement of the M2 anti-inflammatory macrophage phenotype in growth of human gliomas. *J. Pathol.* 216; 15–24.
16. Lisi, L., Ciotti, G. M., Braun, D., Kalinin, S., Currò, D., Dello Russo, C., *et al.* (2017) Expression of iNOS, CD163 and ARG-1 taken as M1 and M2 markers of microglial polarization in human glioblastoma and the surrounding normal parenchyma. *Neurosci. Lett.* 645; 106–112.
17. Liu, P., Wu, X., Liao, C., Liu, X., Du, J., Shi, H., *et al.* (2014) Escherichia coli and Candida albicans induced macrophage extracellular trap-like structures with limited microbicidal activity. *PLoS One* 9; e90042.
18. Martinez, F. O. and Gordon, S. (2014) The M1 and M2 paradigm of macrophage activation: time for reassessment. *F1000Prime Rep.* 6; 13.
19. Mills, C. D., Kincaid, K., Alt, J. M., Heilman, M. J. and Hill, A. M. (2000) M-1/M-2 macrophages and the Th1/Th2 paradigm. *J. Immunol.* 164; 6166–6173.
20. Mohanan, S., Horibata, S., McElwee, J. L., Dannenberg, A. J. and Coonrod, S. A. (2013) Identification of macrophage extracellular trap-like structures in mammary gland adipose tissue: a preliminary study. *Front. Immunol.* 4; 67.
21. Nakanishi, Y., Nakatsuji, M., Seno, H., Ishizu, S., Akitake-Kawano, R., Kanda, K., *et al.* (2011) COX-2 inhibition alters the phenotype of tumor-associated macrophages from M2 to M1 in ApcMin/+ mouse polyps. *Carcinogenesis* 32; 1333–1339.
22. Nayak, D., Roth, T. L. and McGavern, D. B. (2014) Microglia development and function. *Annu. Rev. Immunol.* 32; 367–402.
23. Nishie, A., Ono, M., Shono, T., Fukushi, J., Otsubo, M., Onoue, H., *et al.* (1999) Macrophage infiltration and heme oxygenase-1 expression correlate with angiogenesis in human gliomas. *Clin. Cancer Res.* 5; 1107–1113.
24. Okubo, K., Kurosawa, M., Kamiya, M., Urano, Y., Suzuki, A., Yamamoto, K., *et al.* (2018) Macrophage extracellular trap formation promoted by platelet activation is a key mediator of rhabdomyolysis-induced acute kidney injury. *Nat. Med.* 24; 232–238.
25. O'Malley, J. T., Nadol, J. B. Jr. and McKenna, M. J. (2016) Anti CD163+, Iba1+, and CD68+ Cells in the Adult Human Inner Ear: Normal Distribution of an Unappreciated Class of Macrophages/Microglia and Implications for Inflammatory Otopathology in Humans. *Otol. Neurotol.* 37; 99–108.
26. Onouchi, T., Shiogama, K., Matsui, T., Mizutani, Y., Sakurai, K., Inada, K., *et al.* (2016) Visualization of Neutrophil Extracellular Traps and Fibrin Meshwork in Human Fibrinopurulent Inflammatory Lesions: II. Ultrastructural Study. *Acta Histochem. Cytochem.* 49; 117–123.
27. Onouchi, T., Shiogama, K., Mizutani, Y., Takaki, T. and Tsutsumi, Y. (2016) Visualization of Neutrophil Extracellular Traps and Fibrin Meshwork in Human Fibrinopurulent Inflammatory Lesions: III. Correlative Light and Electron Microscopic Study. *Acta Histochem. Cytochem.* 49; 141–147.
28. Prinz, M. and Priller, J. (2014) Microglia and brain macrophages in the molecular age: from origin to neuropsychiatric disease. *Nat. Rev. Neurosci.* 15; 300–312.
29. REPORT OF BRAIN TUMOR REGISTRY OF JAPAN (2005–2008) 14th Edition. (2017) Brain Tumor Registry of Japan (2005–2008). *Neurol. Med. Chir. (Tokyo)* 57(Suppl 1); 9–102.
30. Sasaki, A. (2017) Microglia and brain macrophages: An update. *Neuropathology* 37; 452–464.
31. Shiogama, K., Onouchi, T., Mizutani, Y., Sakurai, K., Inada, K. and Tsutsumi, Y. (2016) Visualization of Neutrophil Extracellular Traps and Fibrin Meshwork in Human Fibrinopurulent Inflammatory Lesions: I. Light Microscopic Study. *Acta Histochem. Cytochem.* 49; 109–116.
32. Takeya, M. and Komohara, Y. (2016) Role of tumor-associated macrophages in human malignancies: friend or foe? *Pathol. Int.* 66; 491–505.
33. Tamura, R., Ohara, K., Sasaki, H., Morimoto, Y., Kosugi, K., Yoshida, K., *et al.* (2018) Difference in Immunosuppressive Cells Between Peritumoral Area and Tumor Core in Glioblastoma. *World Neurosurg.* 120; e601–e610.
34. Wang, Y., Li, M., Stadler, S., Correll, S., Li, P., Wang, D., *et al.* (2009) Histone hypercitrullination mediates chromatin decondensation and neutrophil extracellular trap formation. *J. Cell Biol.* 184; 205–213.
35. Wong, K. W. and Jacobs, W. R., Jr. (2013) Mycobacterium tuberculosis exploits human interferon γ to stimulate macrophage extracellular trap formation and necrosis. *J. Infect. Dis.* 208; 109–119.
36. Wu, A., Wei, J., Kong, L. Y., Wang, Y., Priebe, W., Qiao, W., *et al.* (2010) Glioma cancer stem cells induce immunosuppressive macrophages/microglia. *Neuro Oncol.* 12; 1113–1125.
37. Xu, S. S., Li, H., Li, T. J., Li, S., Xia, H. Y., Long, J., *et al.* (2021) Neutrophil Extracellular Traps and Macrophage Extracellular Traps Predict Postoperative Recurrence in Resectable Nonfunctional Pancreatic Neuroendocrine Tumors. *Front. Immunol.* 12; 577517.
38. Zhang, Y., Lima, C. F. and Rodrigues, L. R. (2014) Anticancer effects of lactoferrin: underlying mechanisms and future trends in cancer therapy. *Nutr. Rev.* 72; 763–773.